Journal Name

Dynamic Article Links►

Cite this: DOI: 10.1039/c0xx00000x

www.rsc.org/xxxxxx

ARTICLE TYPE

Mesoporous Hybrid Material of Mn_3O_4 Nanoparticles on Nitrogen-doped Graphene for Highly Efficient Oxygen Reduction Reaction

Jingjing Duan[a], Yao Zheng[ab], Sheng Chen[a], Youhong Tang[c], Mietek Jaroniec[d] and Shi Zhang Qiao*[a]

Received (in XXX, XXX) XthXXXXXXXXX 20XX, Accepted Xth XXXXXXXXX 20XX

DOI: 10.1039/b000000x

Hybrid material of Mn_3O_4 nanoparticles on nitrogen-doped graphene was prepared via a solvothermal process and investigated for the first time as a catalyst for oxygen reduction reaction (ORR). Its high ORR activity, excellent durability and tolerance to methanol, make this hybrid material a promising candidate for highly efficient ORR in fuel cells and metal-air batteries.

A major challenge in the commercial development of the key renewable-energy technologies, such as fuel cells and metal-air batteries, is the sluggish oxygen reduction reaction (ORR) on the cathode.[1] Currently, Pt-based materials are considered as the most active ORR catalysts, but their low tolerance to methanol, scarcity of resources and high cost prevent them to be a sustainable solution to low efficient ORR.[2] Therefore, extensive efforts have been undertaken toward development of durable and low cost substitutes with comparable ORR activity to that of commercial Pt/C materials. These efforts are mainly focused on the metal-free catalysts and non-precious metal materials.[3]

Graphene, as a two-dimensional sp^2-hybridized carbon sheet, has attracted a considerable attention either as a non-metal catalyst or as a carbon support for metal catalysts for ORR, because of its excellent electrical conductivity, high surface area and good chemical stability. Recently, doping graphene with heteroatoms like nitrogen has been extensively investigated due to its excellent ORR activity and good durability.[4] Namely, doping graphene with heteroatoms introduces defects in the adjacent sites, which alter asymmetry spin density and charge density, and consequently facilitate the ORR process. Furthermore, since the doped heteroatoms are usually covalently bonded to carbon atoms, their effect does not fade even during a long time operation, which assures their great durability.[4]

Alternatively, a broad range of catalysts based on non-precious metal oxides (Fe_3O_4, Co_3O_4, etc.) have been actively pursued as ORR electrocatalysts because of their low cost, abundance and environmental compatibility.[5] In particular, Mn_3O_4 with unique mixed-valence state has been an active catalyst in several redox reactions.[6] The coexistence of Mn^{2+}, $Mn^{3+}$and Mn^{4+} may facilitate the formation of defects (vacancies, electrons and holes), which would affect the electronic distribution between Mn_3O_4 and graphene. Nevertheless, as in the case of other nanoparticles, nanostructured supports such as graphene are needed to prevent Mn_3O_4 nanoparticles from dissolution and agglomeration during catalytic processes.[7] It was shown recently that metal oxides nanoparticles on doped carbons exhibited an enhanced ORR activity.[5b, 8] However, as far as we know, a hybrid material composed of Mn_3O_4 nanoparticles and nitrogen-doped graphene has not been investigated yet as an ORR catalyst presumably due to the low electrical conductivity of Mn_3O_4.[9]

Here we demonstrate that a new type catalyst, composed of Mn_3O_4 nanoparticles and nitrogen-doped graphene, shows a high ORR activity, excellent durability and is fully tolerant to methanol. The mesoporous architecture of this hybrid was shown to be favourable for oxygen adsorption and transport during ORR process.[6, 9] Also, Mn_3O_4 nanoparticles may be partially reduced by nitrogen-doped graphene in the hybrid according to previous reports.[10] Additionally, newly formed metal-N-C and metal-O-C bonds can provide strong coupling between metal and graphene, thus preventing nanoparticles from agglomeration, and improving charge transfer and electroconductivity.[8, 10c, 11]

As shown in Scheme 1, the defects and functional groups on adapted graphene oxide sheets (GO) can serve as nucleation and anchoring sites for nanoparticles. GO was partly reduced (denoted as prGO) by ammonia in ethylene glycol at 80 °C for 10 hrs. Meantime, Mn_3O_4 nuclei were formed via heterogeneous nucleation on GO. The product was further solvothermally treated in an autoclave at 150 °C for 3 hrs, prGO was reduced and nitrogen from ammonia was doped to GO. At the final stage crystallization of Mn_3O_4 nuclei was completed, forming Mn_3O_4 nanoparticles on nitrogen-doped graphene (denoted as MNG).

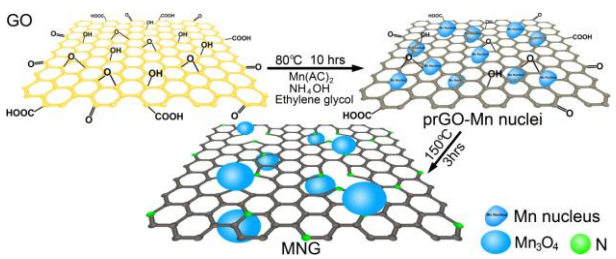

Scheme 1 Schematic illustration of the formation mechanism of MNG.

As shown in Fig. S1a and b in ESI, the as-prepared GO is in the form of very thin carbon sheets with wrinkles. According to its AFM image and height distribution curve (Fig. S1c and d in ESI), the thickness is ~3.5 nm, about 4 layers of carbon sheets. The as-prepared Mn_3O_4 nanoparticles (about 20 nm) in the hybrid were regularly dispersed on N-doped graphene sheets (Fig. 1a). In contrast, Mn_3O_4 nanoparticles prepared by the same process

but without GO (denoted as MPs, Fig. S2a in ESI) agglomerated severely. The sample obtained without Mn precursor (denoted as NG, Fig. S2b in ESI) showed no obvious change as compared to GO. The regularity and very good dispersion of Mn_3O_4 nanoparticles on N-graphene is highly advantageous for the ORR process.

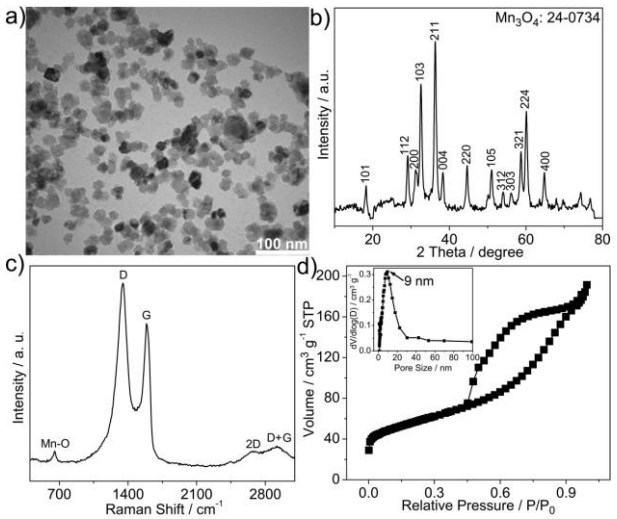

Fig.1(a) TEM image, (b) XRD pattern, (c) Raman spectrum, (d) nitrogen adsorption-desorption isotherm and pore size distribution curve (inset) for the MNG hybrid material studied.

A noticeable reduction in the sheet spacing as evidenced by change in (002) reflection on the XRD patterns of GO and NG (Fig. S3a and b in ESI) suggests the removal of plane oxygen atoms. The content of oxygen in NG was examined by XPS to be 15.2% (Fig. S4 in ESI). The XRD pattern of MNG (Fig.1b) is similar to that of MPs (Fig. S3c in ESI), which can be assigned to hausmannite Mn_3O_4 ($I4_1/amd$, $a_0=b_0=5.76$ Å, and $c_0=9.47$ Å; JCPDS card no. 24-0734). Raman spectrum shows signals of Mn-O band (650 cm^{-1}) from Mn_3O_4, and D band (1350 cm^{-1}), G band (1588 cm^{-1}), 2D band (2675 cm^{-1}) and combination of D+G band (2935 cm^{-1}) from graphene (Fig. 1c). The high ratio of I_D/I_G (1.26) clearly indicates the presence of structure defects.[12] The nitrogen adsorption isotherm measured on MNG (Fig. 1d) is type-IV with a distinct hysteresis loop and the pore size distribution curve is centred at ~9 nm (inset in Fig. 1d), both suggesting the mesoporous architecture of this hybrid material.[13] The BET specific surface area and total pore volume of MNG were estimated to be ~190 $m^2\ g^{-1}$ and 0.30 $cm^3\ g^{-1}$ respectively, both higher than those of MPs (~90 $m^2\ g^{-1}$ and 0.23 $cm^3\ g^{-1}$, Fig. S5a and b in ESI) and lower than those of NG (~470 $m^2\ g^{-1}$ and 0.47 $cm^3\ g^{-1}$, Fig. S5c and d in ESI), respectively. In this hybrid, Mn_3O_4 nanoparticles have acted as spacers to create mesoporous architecture between the inter-layers of N-doped graphene sheets, which would facilitate the molecular transport during ORR.

The XPS survey of MNG and Mix (0-1000 eV) both show the existence of manganese, carbon, oxygen and nitrogen (Fig. 2a and Fig. S6a in ESI). The deconvolution of N spectrum in MNG (Fig. 2b) indicates the presence of pyridinic N (398.8 eV), pyrrolic N (400.4 eV) and graphitic N (401.7 eV). A $2p_{3/2}$-$2p_{1/2}$ doublet at 641.7 and 653.3 eV with a splitting width of 11.6 eV in Mn 2p spectrum of MNG is observed (Fig. 2c).[14] The deconvolution of C in MNG is shown in Fig. S7 (ESI) and the calculated N/C ratio in MNG is 2.2%. Moreover, there is a downshift of 1.4 eV in Mn $2P_{3/2}$ peak of MNG as compared to Mix, probably due to the newly formed metal-N-C and metal-O-C bonds (Fig. S6b in ESI).[8, 10c, 11] In the FTIR spectra (Fig. 2d), new peaks are identified at 1560 and 1020 cm^{-1} both in NG and MNG, which can be assigned to sp^2 bonded C-N.[15] The peaks at around 630, 502 and 458 cm^{-1} in MNG are assigned to tetrahedral and octahedral Mn-O bands. Furthermore, the mass ratio of Mn_3O_4 in MNG was measured to be ~74% using TGA (Fig. S8 in ESI).

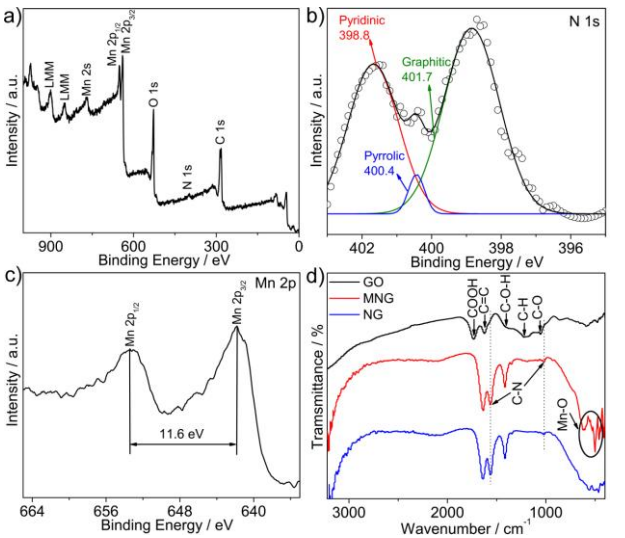

Fig.2 (a) XPS survey (0-1000 eV), (b) N spectrum and (c) Mn 2p spectrum of MNG; (d) FTIR spectra of GO, MNG and NG.

Basically, the cathodic ORR proceeds either through high efficient four electron process, or slow two electron pathway. The cyclic voltammetry (CV) of MPs, NG, Mix, MNG and commercial Pt/C were first examined on a rotating disk electrode (RDE) both in O_2 and N_2-saturated 0.1M KOH solution (Fig. 3a and Fig. S9 in ESI). CV curves recorded in N_2-saturated electrolyte show no ORR peaks. The anodic peaks at ~0.1V in Fig. 3a correspond to the redox cycling of MnO_2 phase on the surface of MNG.[16] CV of MPs in O_2-saturated electrolyte shows two peaks with one at -0.48 V and the other at -0.83 V, corresponding to the two step-two electron process.[17] But CV of MNG in O_2-saturated electrolyte displays one peak at -0.3 V, positive as compared to that of NG (-0.35V) and Mix (-0.34 V), suggesting a four electron process.[9, 17-18]

The linear sweeping voltammograms (LSVs) recorded on RDE at 1600 rpm in O_2-saturated 0.1 M KOH were compared in Fig. 3b. The LSV of MNG shows a positive onset-potential of -0.09 V and a current density of 3.7 mA cm^{-2} at -0.4 V, very close to those of Pt/C (-0.07 V and 4.2 mA cm^{-2}) and higher than those of NG (-0.12 V and 2.58 mA cm^{-2}), Mix (-0.16 V and 2.57 mA cm^{-2}) and MPs (-0.32 V and 0.45 mA cm^{-2}). The as-prepared NG here exhibits better ORR performance than previously reported N-doped graphene structures.[19] The positive onset-potential as well as the high current density of MNG suggest its facile and excellent ORR activity, as evidenced by CV data.

To obtain further information about ORR kinetics, detailed LSVs and quantitative Koutecky-Levich plots (K-L, J^{-1} vs. $\omega^{-1/2}$)

were shown in Fig. 3c and d and Fig. S10 in ESI. The electron transfer number of MNG (n, estimated from the slopes of linear K-L plots) is 3.85 at -0.4 V, higher than that of NG (3.18), Mix (3.52) and close to Pt/C (3.99). The enhanced ORR activity of MNG as compared to Mix may be related to the reduced electrochemical impedance of MNG (Fig. S11 in ESI). N values estimated from rotating ring-disk electrode voltammograms are shown in Fig. S12 (ESI), with n of MNG as 3.6 at -0.4 V (Pt/C: 3.9 at -0.4 V) higher than that of NG (3.2 at -0.4 V).[8-9] The good linearity of K-L plots and high electron transfer number further confirm the high ORR efficiency of MNG.

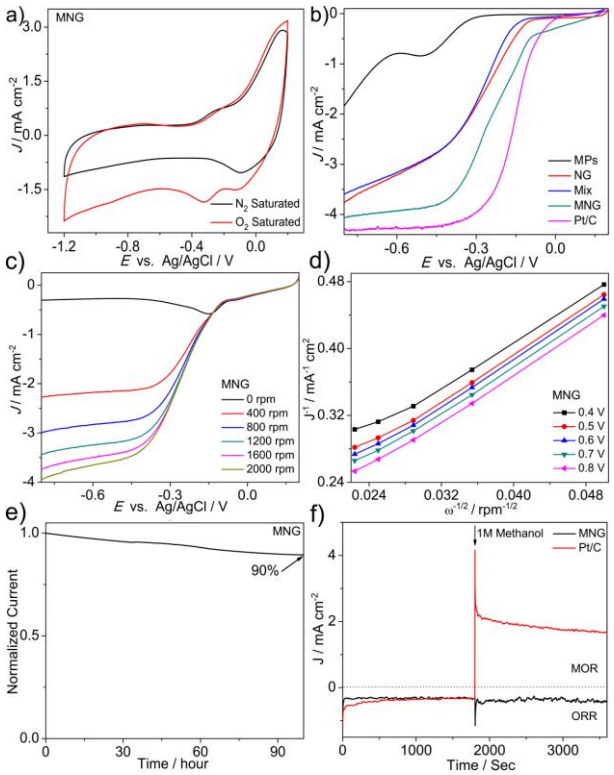

Fig.3 (a) CV curves of MNG in N_2 and O_2-saturated 0.1 M KOH; (b) LSVs at 1600 rpm with a sweep rate of 5 mV s^{-1} recorded on Pt/C, MNG, Mix, NG and MPs in O_2-saturated electrolyte; (c) LSVs at different rotating speeds and (d) calculated K-L plots of MNG; (e) i-t of MNG at -0.3 V. (f) i-t of Pt/C and MNG at -0.35 V before and after the addition of 1M methanol. Catalyst loading was 0.2 mg cm^{-2} for all samples.

Furthermore, long-time stability was evaluated using chronoamperometric response (i-t) in O_2-saturated 0.1M KOH (Fig. 3e). MNG exhibited an excellent stability, retaining 90% of the initial current even after 100 hrs at -0.3 V; while Pt/C catalyst lost almost 50% of its initial current only after 60 hrs at -0.3 V.[20] Mix sample lost 25% of initial current during 2 hrs (Fig. S13 in ESI). In addition, the tolerance to methanol of MNG was measured to test its selectivity towards ORR with the addition of 1M methanol. The current density of MNG showed no obvious change after the addition of methanol, suggesting a high selectivity to ORR which is promising in direct methanol fuel cells. However, Pt/C exhibited a distinct methanol oxidation reaction after introduction of methanol.[20] Moreover, the MNG electrocatalyst can also survive in highly corrosive electrolyte like 1 M and 6M KOH, demonstrating high activity, favourable kinetics and excellent stability (Fig. S14 in ESI).

In summary, a new type non-precious ORR catalyst composed of Mn_3O_4 nanoparticles and nitrogen-doped graphene is reported which shows a competitive ORR activity, excellent durability, and high selectivity. The mesoporous architecture of the hybrid is advantageous for oxygen adsorption and molecular transport during catalytic process. Doping graphene with nitrogen through a liquid phase process is much safer and lower energy-cost as compared to the widely used vapour-assisted synthesis. Importantly, the covalent bonding between Mn_3O_4 and graphene guarantees a durable and facile ORR process. The low cost, highly efficient, durable and highly selective ORR catalyst may provide a potential solution to the sluggish ORR, which is important to the development of new energy conversion systems.

Notes and references

[a] *School of Chemical Engineering, University of Adelaide, Adelaide, SA 5005, Australia. Fax: +61 8 83034373; Tel: +61 8 83136443; E-mail: s.qiao@adelaide.edu.au*

[b] *Australian Institute for Bioengineering and Nanotechnology, University of Queensland, Brisbane, QLD 4072,Australia.*

[c] *Centre for Nano Scale Science and Technology, and School of Computer Science, Engineering, and Mathematics, Flinders University. Adelaide, SA 5042, Australia.*

[d] *Department of Chemistry and Biochemistry, Kent State University, Kent, Ohio 44242,USA.*

† Electronic Supplementary Information (ESI) available: [details of any supplementary information available should be included here]. See DOI: 10.1039/b000000x/

1. (a) M. K. Debe, *Nature*, 2012, **486**, 43; (b) R. Cao, J.-S. Lee, M. Liu and J. Cho, *Adv. Energy Mater.*, 2012, **2**, 816.
2. D. Wang, H. L. Xin, R. Hovden, H. Wang, Y. Yu, D. A. Muller, F. J. DiSalvo and H. D. Abruña, *Nat. Mater.*, 2013, **12**, 81.
3. (a) Y. Li, W. Zhou, H. Wang, L. Xie, Y. Liang, F. Wei, J. C. Idrobo, S. J. Pennycook and H. Dai, *Nature Nanotech.*, 2012, **7**, 394; (b) I. Y. Jeon, H. J. Choi, S. M. Jung, J. M. Seo, M. J. Kim, L. Dai and J. B. Baek, *J. Am. Chem. Soc.*, 2013, **135**, 1386.
4. D. Geng, Y. Chen, Y. Chen, Y. Li, R. Li, X. Sun, S. Ye and S. Knights, *Energy Environ. Sci.*, 2011, **4**, 760.
5. (a) Y. Liang, H. Wang, P. Diao, W. Chang, G. Hong, Y. Li, M. Gong, L. Xie, J. Zhou, J. Wang, T. Z. Regier, F. Wei and H. Dai, *J. Am. Chem. Soc.*, 2012, **134**, 15849; (b) Z. S. Wu, S. Yang, Y. Sun, K. Parvez, X. Feng and K. Mullen, *J. Am. Chem. Soc.*, 2012, **134**, 9082.
6. Z. R. Tian, W. Tong, J. Y. Wang, N. G. Duan, V. V. Krishnan and S. L. Suib, *Science*, 1997, **276**, 926.
7. S. Guo, S. Zhang, L. Wu and S. Sun, *Angew. Chem. Int. Ed.*, 2012, **51**, 11770.
8. Y. Liang, Y. Li, H. Wang, J. Zhou, J. Wang, T. Regier and H. Dai, *Nat. Mater.*, 2011, **10**, 780.
9. Y. Tan, C. Xu, G. Chen, X. Fang, N. Zheng and Q. Xie, *Adv. Funct. Mater.*, 2012, **22**, 4584.
10. (a) M. Seredych and T. J. Bandosz, *J. Mater. Chem.*, 2012, **22**, 23525; (b) H. Yang, J. Jiang, W. Zhou, L. Lai, L. Xi, Y. M. Lam, Z. Shen, B. Khezri and T. Yu, *Nanoscale Res. Lett.*, 2011, **6**, 531; (c) J. Wang, J. Zhou, Y. Hu and T. Regier, *Energy Environ. Sci.*, 2013, **6**, 926.
11. (a) Y. Liang, Y. Li, H. Wang and H. Dai, *J. Am. Chem. Soc.*, 2013, **135**, 2013; (b) Y. Liang, H. Wang, J. Zhou, Y. Li, J. Wang, T. Regier and H. Dai, *J. Am. Chem. Soc.*, 2012, **134**, 3517.
12. J. Liu, H. Cai, X. Yu, K. Zhang, X. Li, J. Li, N. Pan, Q. Shi, Y. Luo and X. Wang, *J. Phys. Chem. C*, 2012, **116**, 15741.
13. M. Kruk and M. Jaroniec, *Chem. Mater.*, 2001, **13**, 3169.
14. J. W. Lee, A. S. Hall, J.-D. Kim and T. E. Mallouk, *Chem. Mater.*, 2012, **24**, 1158.
15. (a) Z. Lin, M.-k. Song, Y. Ding, Y. Liu, M. Liu and C.-p. Wong, *Phys. Chem. Chem. Phys.*, 2012, **14**, 3381; (b) P. Wu, Y. D. Qian, P. Du, H. Zhang and C. X. Cai, *J. Mater. Chem.*, 2012, **22**, 6402.
16. F. H. B. Lima, M. L. Calegaro and E. A. Ticianelli, *Electrochimica Acta*, 2007, **52**, 3732.
17. Y. Zheng, Y. Jiao, J. Chen, J. Liu, J. Liang, A. Du, W. Zhang, Z. Zhu, S. C. Smith, M. Jaroniec, G. Q. Lu and S. Z. Qiao, *J. Am. Chem. Soc.*, 2011, **133**, 20116.
18. K. L. Pickrahn, S. W. Park, Y. Gorlin, H.-B.-R. Lee, T. F. Jaramillo and S. F. Bent, *Adv. Energy Mater.*, 2012, **2**, 1269.
19. (a) Y. Zhang, K. Fugane, T. Mori, L. Niu and J. Ye, *J. Mater. Chem.*, 2012, **22**, 6575; (b) Y. Zhao, C. Hu, Y. Hu, H. Cheng, G. Shi and L. Qu, *Angew. Chem. Int. Ed.*, 2012, **51**, 11371.
20. J. Liang, Y. Zheng, J. Chen, J. Liu, D. Hulicova-Jurcakova, M. Jaroniec and S. Z. Qiao, *Angew. Chem. Int. Ed.*, 2012, **51**, 3892.